Design of Frequency Reconfigurable Multiband Compact Antenna using two PIN diodes for WLAN/WiMAX Applications

Y. I. Abdulraheem, G. A. Oguntala, A. S Abdullah, H. J. Mohammed, R. A. Ali, R. A. Abd-Alhameed and J. M. Noras

Abstract:

In this paper, we present a simple reconfigurable multiband antenna with two PIN diode switches for WiMAX/WLAN applications. The antenna permits reconfigurable switching in up to ten frequency bands between 2.2 GHz and 6 GHz, with relative impedance bandwidths of around 2.5% and 8%. The proposed antenna has been simulated using CST microwave studio software and fabricated on an FR-4 substrate. It is compact, with an area of 50 × 45 mm^2, and has a slotted ground substrate. Both measured and simulated return loss characteristics of the optimized antenna show that it satisfies the requirement of 2.4/5.8 GHz WLAN and 3.5 GHz WiMAX antenna applications. Moreover, there is good agreement between the measured and simulated result in terms of radiation pattern and gain.

Keywords: Electronic tuning, PIN diode switch, frequency reconfigurable antenna, multiband, frequency optimization

I. INTRODUCTION

The proliferation in demand for reliable, high performance cognitive radio systems and broadband services has invariably necessitated the use of reconfigurable antennas. In most wireless communication systems, spread spectrum signalling is used in mitigating crosstalk interference from users using the same channel in multiple access communication. This is due to its high efficiency, resulting in reduced susceptibility to multipath fading and improved security of data from intruders, thereby making spread spectrum signals hard to jam [1].

However, spread spectrum signals are characterized by their relatively large bandwidths which often require the use of an antenna with the capability of operating within such bandwidths. Spread spectrum signal are most applicable in wireless local area networks (WLAN) and worldwide interoperability for microwave access (WiMAX) [2].

Reconfigurable antennas are dynamic antennas with the capability of modifying their properties such as radiation pattern, polarization and frequency with changing system requirements or environmental conditions in a controlled and reversible manner [3, 4]. In particular, frequency reconfigurability in antennas is beneficial for diverse applications, as it reduces the bandwidth requirement of spread spectrum signals. This is due to the fact that wireless applications will not need to cover all operating frequencies simultaneously, which in effect will ameliorate any restriction on antennas and improve their functionalities without increasing their size and complexity [5, 6]. Other desirable characteristics of frequency reconfigurable antennas include their miniaturized size, low cost and use for a variety of applications resulting in their integration into most modern wireless systems [7].

Several authors have achieved frequency reconfigurability by adjusting the effective length of an antenna either by adding or removing part of its length through the use of different methods such as RF-MEMS for frequency tuning [8-10]. The use of varactor diodes for redirecting surface currents, thereby allowing smooth frequency change with change in capacitance, has been reported in [11], and the use of RF PIN diodes for tuning frequency bands in [12-15]. Antenna frequency reconfigurability using RF-MEMS exhibits lower loss and higher Q factors in comparison with varactor and PIN diodes [16]. On the other hand, PIN diodes have low cost, relatively high power handling capability, faster switching speed, good isolation, low insertion loss and are easier to fabricate for optimal performance [17]. In addition, earlier work reports that biasing circuits often become complicated whenever vias and bias lines are required for PIN diode activation, which in effect often degrades the

performance of antennas [18-20]. Hence, in this work we integrate the biasing circuit on the same antenna plane for circuit simplicity since no vias will be used, and the PIN diodes are used to control the effective electrical length of the antenna.

Thus, this paper presents a compact, multiband antenna with an overall dimension of 50 × 45 x 1.6 mm^3. The major advantage of the proposed antenna comes from its ability to resonate at ten different frequencies. Switches using PIN diodes (SMP1320-079), located in the slot of the antenna, control the length of the slot, thereby achieving ten different frequencies ranging from 2.2 to 6 GHz. The detailed design of the proposed antenna is described in Section II. In Section III, we investigate the performance of the antenna, present simulated and measured results. Section IV concludes the paper.

II. ANTENNA DESIGN AND CONFIGURATION

A. Antenna geometry

This sub-section briefly explains the antenna structure. The antenna is designed on an FR-4 substrate with a thickness h of 1.6 mm, tangential loss of 0.02 and a relative permittivity ε_r of 4.3. Simulations were performed using Computer Simulation Technology (CST) software. The geometry of the antenna is illustrated in Fig. 2. (a) and (b) which illustrate its front and back views. The antenna has two slots in the ground plane and is offset fed by a 50 Ω microstrip feed line positioned on the opposite side of the substrate. The overall dimensions of the antenna are W_g = 50 mm and L_g = 45 mm, as shown in Table 1. The length of the microstrip feed line L_3 = 4.85 mm while the width is 1 mm. The first switch, PIN diode 1, is placed at the middle of the bottom slot, while the second switch, PIN diode 2, is placed at the top slot of the antenna at a distance of L_9 = 1 mm. Introducing the slot or altering the length of the patch changes the current distribution, which potentially improves the impedance matching of the antenna in different frequency bands.

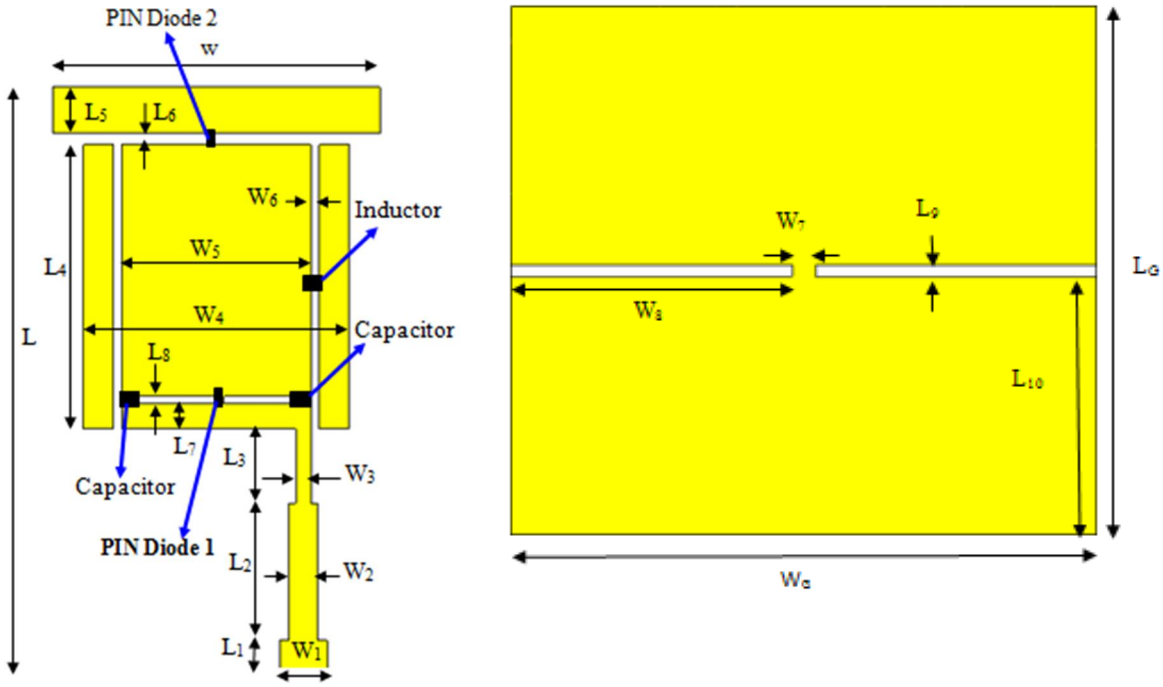

(a) (b)

Fig. 2: Geometry of the antenna; (a) Front view, (b) Back view.

Table 1: Detailed antenna parameters (Units in mm).

W	W_1	W_2	W_3	W_4	W_5	W_6
21.4	3.11	1.87	1	17.4	12.4	0.5
W_7	W_8	h	L	L_1	L_2	L_3
2	24	1.6	38.2	2	9	4.85
L_4	L_5	L_6	L_7	L_8	L_9	L_{10}
18.58	3	0.77	1.65	0.5	1	22
$W_g \times L_g$						
50 × 45						

B. Design Methodology

The loading of two identical slots in the radiating patch causes meandering of the excited patch surface currents, which results in a new resonant frequency at 5.2 GHz with 3.8% bandwidth. This new feature is useful for WiMAX applications, while the resonant frequency and bandwidth of the fundamental frequency at 2.4 GHz remain unchanged. The third resonant frequency has 2.5% bandwidth at 4.7 GHz. In addition, by making another two parallel and identical slots in the radiating patch, a new resonant frequency

was achieved at 3.6 GHz with 4% bandwidth, suitable for operations in the licensed band for WLAN applications. Furthermore, embedding meandering slots in the antenna ground plane enhances impedance bandwidth and antenna gain. The other observed resonant frequencies are 4.3 GHz and 5.2 GHz, with impedance bandwidths of 2.3% and 2.9% respectively. We adopted various steps in order to overcome constraints imposed by the radiating environment. A flowchart representing these steps taken in achieving the desired capability is shown in Fig. 1.

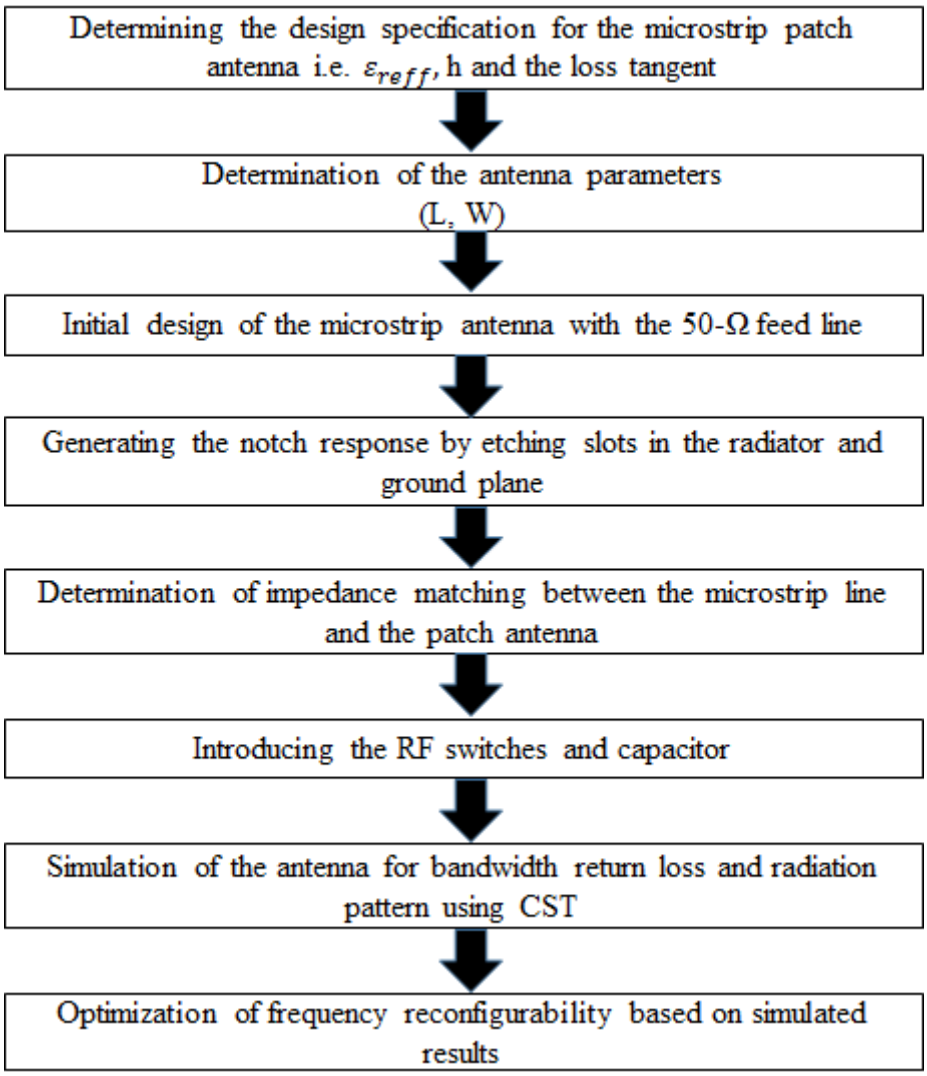

Fig. 2: Flowchart of antenna design methodology

c. Switch design

In order to implement electronic reconfigurability, the ideal shunt switches must be replaced with PIN diodes. These diodes are particularly appropriate for the reconfigurability we want to achieve due to their compact size, high switching speed, reliability, and small resistance and capacitance in the ON and OFF states. The circuit connection of the PIN diode as a shunt is shown in Fig. 3. (a) and (b) for both the ON and the OFF states respectively. The reactive components C_T and L_S model the packaging effect, while others model the electric properties of the diode junction in the ON and OFF conditions. From the manufacturer's data, the SMP1320-079 circuit parameters are C_T = 0.3 pF and R_S = 0.9 Ω. L_S = 0.7 nH, parasitic inductance resulting from the packaging and the value of R_p is assumed higher than the reactance of C_T, thus it is neglected from the equivalent model.

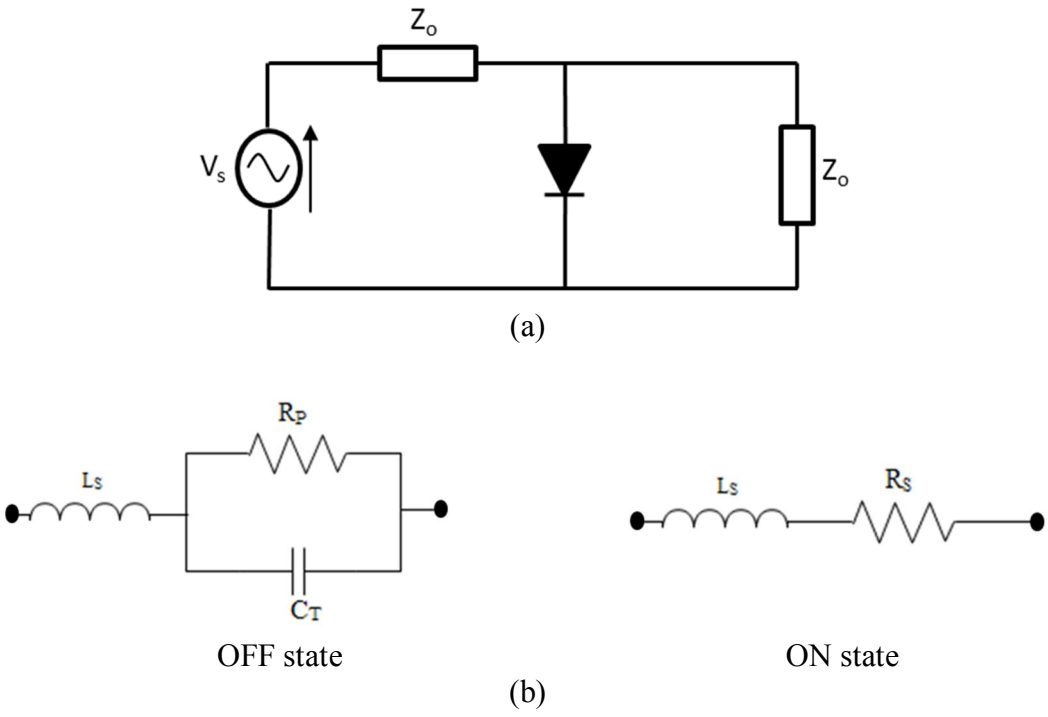

Fig. 3: PIN diode connected as a shunt switch (a), and RF equivalent circuit models for PIN diodes (b).

The corresponding biasing circuit is shown in the antenna layout in Fig. 4. It should be noted that the RF choke and the DC blocking capacitors are set to 10 nH and 10 pF in the modelling process. The chip capacitor and chip RF choke are provided by Murata. The PIN diodes are

forward biased with a voltage of 1 V and a 100 mA current. Fig. 5. (a) and (b) show the front and back view of the prototype.

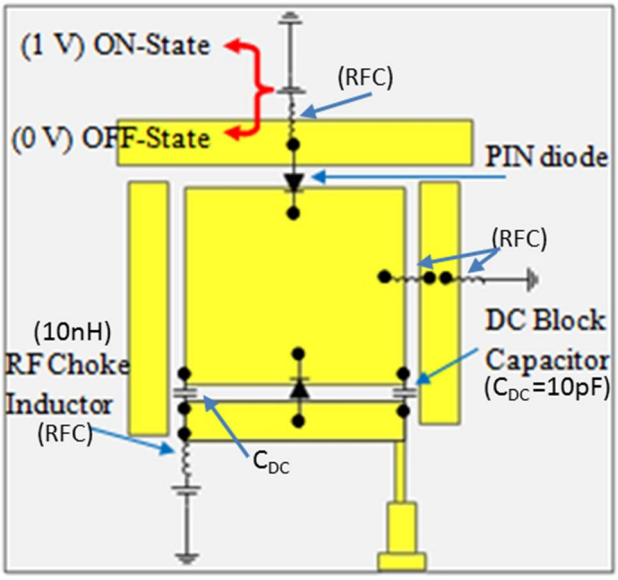

Fig. 4: Antenna layout with biasing circuit.

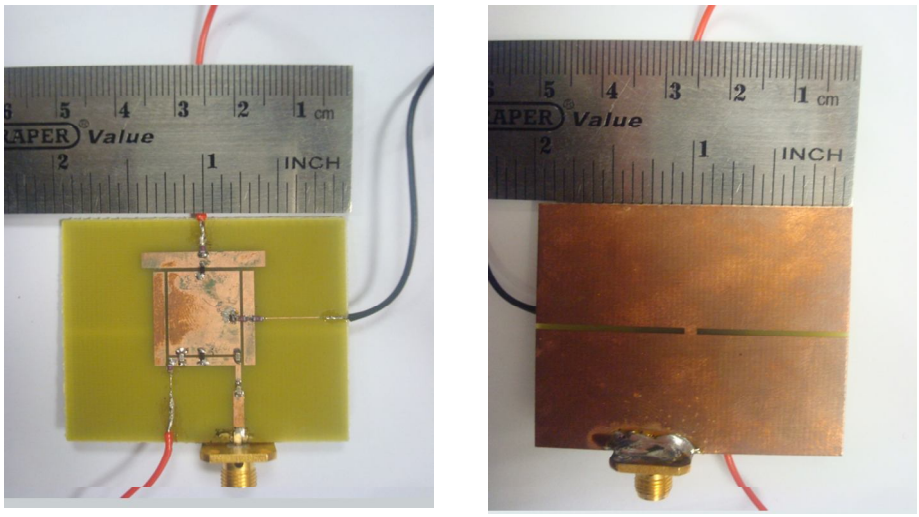

(a) (b)

Fig. 5: Antenna prototype with biasing lines (a) front view (b) back view.

The SPICE model of CST software has hybrid EM-circuit co-simulation built in, which does not take into account the inductance L_S, due to the packaging of the diode, which needs to be included so that simulated and measured results can be properly compared. A model including that parameter is used, giving better agreement with the measured results.

However, when the co-simulation uses a fully-fledged circuit simulator, the effect of a more detailed SPICE diode model for the diode is achieved by replacing the resistor or capacitor by the SPICE model, which can be controlled by a biasing voltage, as shown in Fig. 6.

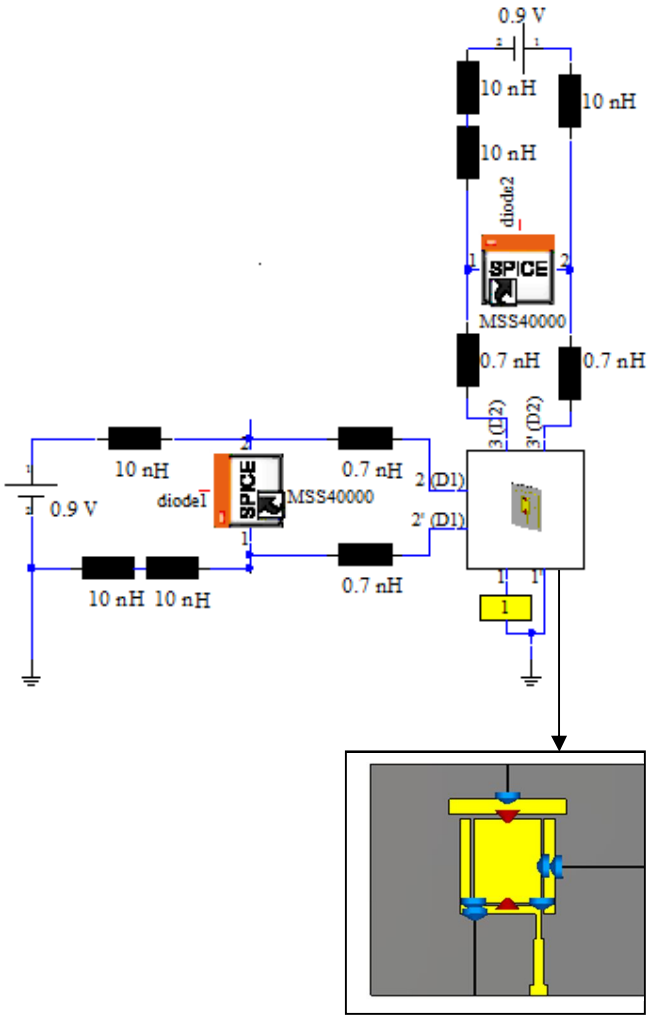

Fig. 6: Hybrid EM-circuit co-simulation for the antenna.

III. RESULT AND DISCUSSION

Simulating the reconfigurable antenna with the PIN diode equivalent circuit is important in order to achieve good agreement with measurements carried out as shown in Fig. 6. The antenna was simulated using CST Microwave Studio, with SPICE models of the diodes, capacitors and inductors incorporated into the CST Design Studio.

Return losses, input resistance and reactance, radiation patterns and gains were simulated and measured with different DC biasing across the PIN diodes: the results obtained from the CST simulation and measurements from the HP 8510C network analyser show reasonable agreement.

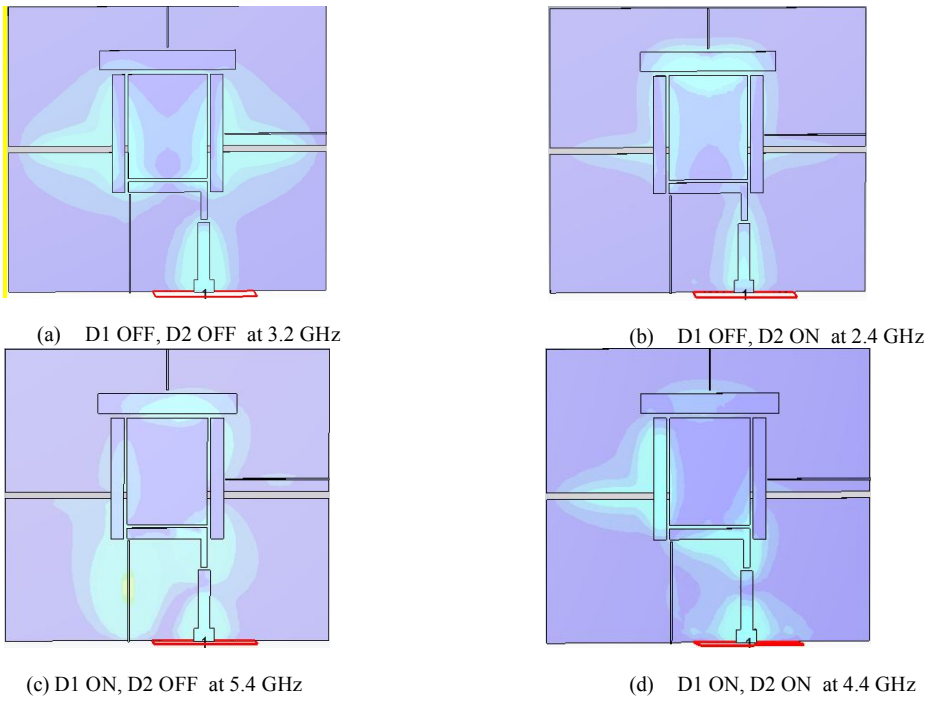

(a) D1 OFF, D2 OFF at 3.2 GHz (b) D1 OFF, D2 ON at 2.4 GHz

(c) D1 ON, D2 OFF at 5.4 GHz (d) D1 ON, D2 ON at 4.4 GHz

Fig. 7. Current distributions of the antenna at different resonant frequencies

i. Surface Current Distributions

In order to understand the mechanism of the antenna operation, it is imperative to analyse the current distributions related to the antenna switching states. Since the two RF PIN diodes D1 and D2 provide four possible switching configurations, the current distribution in the antenna varies as D1 and D2 are activated, as seen in Fig. 7. When D1, D2 are OFF, the lower section of the patch is excited by the feed which allows maximum current distribution at the edges of the patch thereby making the antenna resonate at 3.2 GHz and 5.3 GHz. When D1 is OFF and D2 is ON, current moves more to the top strip of the patch which makes the antenna resonate

at 2.4 GHz. 4.5 GHz and 4.8 GHz respectively. When D1 is ON and D2 is OFF, current is not completely isolated from the top section of the patch which makes the antenna resonate at 3.3 GHz and 5.4 GHz. However, when both diodes are ON, current flows at both the top and bottom of the patch which makes the antenna resonate at three frequencies, 2.2 GHz, 4.48 GHz and 5.3 GHz.

ii. *Reflection Coefficients*

The two PIN diodes provide four possible switching states, (D1 OFF, D2 OFF), (D1 OFF, D2 ON), (D1 ON, D2 OFF) and (D1 ON, D2 ON). The diodes tune the antenna over a frequency range of 2.2–6.0 GHz. CST microwave studio software is used to find the impedance bandwidth (for S_{11} < -10 dB) in the four switching states. Subsequently, the antenna was fabricated and analysed using a vector network analyser to validate the S_{11} values at the different states. Fig. 8 presents the simulation and the measurement of the reflection coefficients for two states; these are (D1 OFF, D2 OFF) and (D1 OFF, D2 ON). Similarly Fig. 9 represents the other two states (i.e., (D1 ON, D2 OFF) and (D1 ON, D2 ON)). It can be observed that at all resonant frequencies, the reflection coefficient is better than -30 dB. The simulated and measured results were reasonable, with small differences at higher resonances frequencies for the two states, (D1 OFF, D2 OFF at the 2nd resonance) and (D1 ON, D2 OFF at the third resonance).

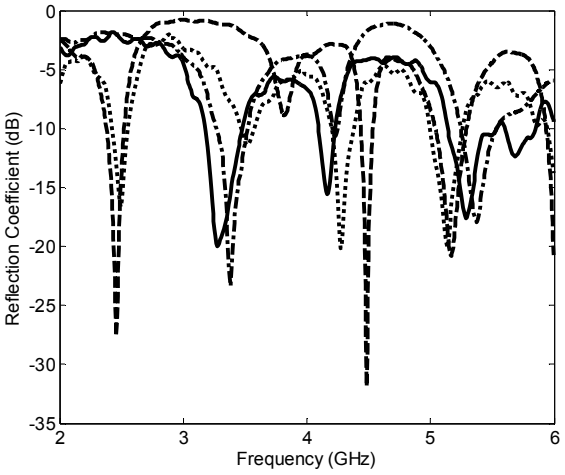

Figure 8: Simulated and measured reflection coefficient:
(D1 OFF, D2 OFF) measured solid line
(D1 OFF, D2 OFF) simulated dotted/dashed line
(D1 OFF, D2 ON) measured dotted line
(D1 OFF, D2 ON) simulated dashed line.

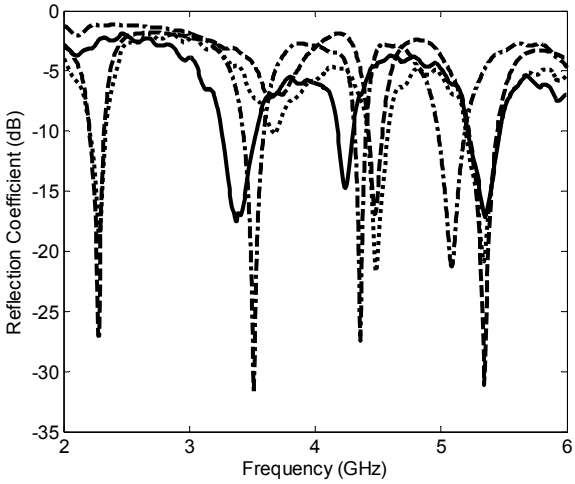

Figure 9: Simulated and measured reflection coefficient:
(D1 ON, D2 OFF) measured solid line
(D1 ON, D2 OFF) simulated dotted/dashed line
(D1 ON, D2 ON) measured dotted line
(D1 ON, D2 ON) simulated dashed line.

Table 2 shows the resonance frequency and the corresponding impedance bandwidth (for reflection coefficient S_{11} < -10 dB) for each of the four states provided by the two PIN diodes. Equation (2) was used in calculating the bandwidth, as given by:

$$BW_{narrowband} = \left(\frac{f_H - f_L}{f_C}\right) * 100 \qquad (2)$$

Table 2: Resonant frequencies and their estimated impedance bandwidths

Switch configuration		**f_r / GHz**	**Impedance bandwidth %**
Diode 1	**Diode 2**		
0	1	2.4	4.5
		4.2	2.5
		5.1	4.8
1	0	3.3	5.8
		5.4	5.7
0	0	3.2	6
		5.3	4
1	1	2.2	3.5
		4.48	2.4
		5.3	4.4

*** 1 = ON, * 0 = OFF**

iii. Resistance and Reactance

Fig. 10 shows the variations of the input resistance and reactance at the input port of the proposed antenna for the following diodes states; (a) D1 OFF, D2 OFF, (b) D1 OFF, D2 ON, (c) D1 ON, D2 OFF, and (d) D1 ON, D2 ON. When the diodes are OFF, there is coupling provided by the two parallel capacitors (each providing an equivalent 150 ohms reactance each at 3.5 GHz) located at the lower section, in addition to the coupling of the lower feeding stripline to the patch. It should be noted that the total length available for the patch is around 20 mm which results in some mismatch around that frequency. However, for most frequencies the simulated and measured results show good agreement.

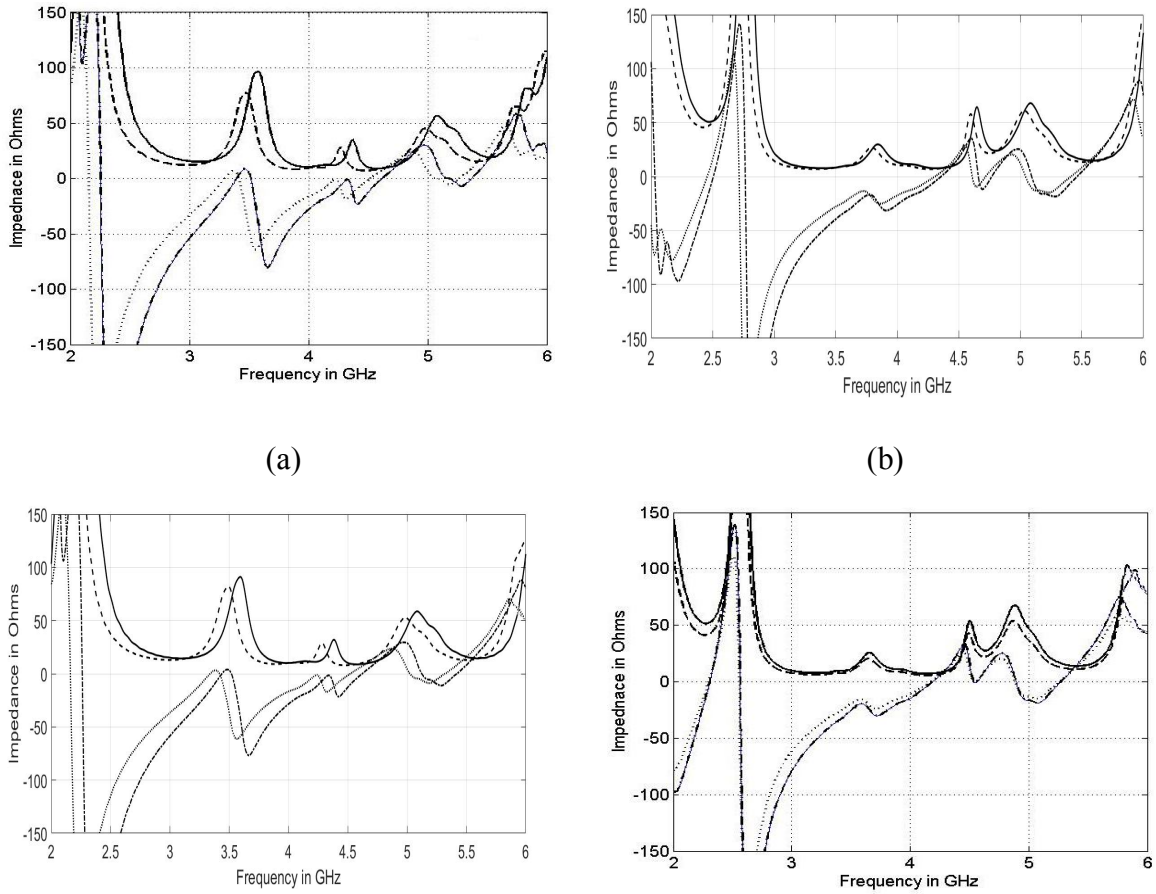

Fig. 10: The simulated and the measured input resistance and reactance at the input port; impedance; (simulated R = solid line, measured R = dashed line, simulated X =

dashed/dotted line and measured X = dotted line), for the following diodes states:

(a) D1 is OFF and D2 is OFF
(b) D1 is OFF and D2 is ON
(c) D1 is ON and D2 is OFF
(d) D1 is ON and D2 is ON

iv. Radiation patterns

Fig. 11 shows the effects of the PIN diodes on the measured and simulated patterns of the antenna in different switching states, with different resonant frequencies across the operating bandwidth. Here, E_φ and E_θ represent the co-polarization and cross-polarization characteristics, respectively. The yz-coordinates were taken into account as the E-plane, and xz-coordinates as the H-plane.

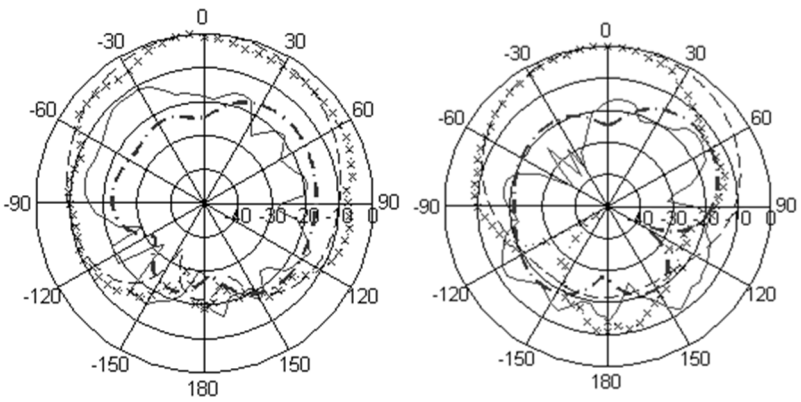

1: (D1 ON, D2 ON) state at 5.3 GHz

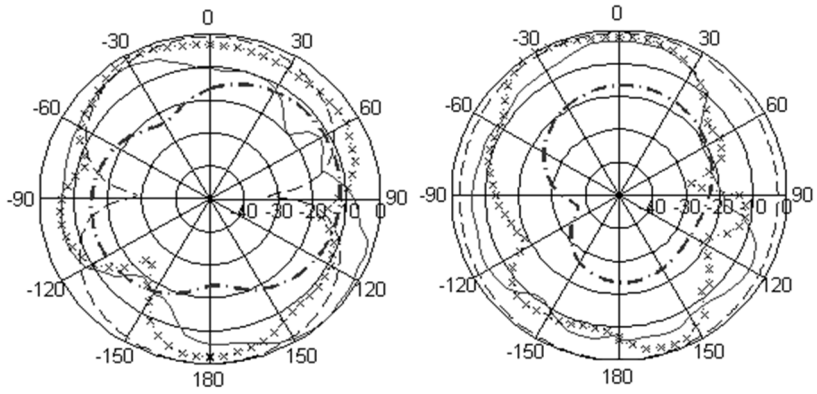

2: (D1 OFF, D2 ON) state at 2.4 GHz

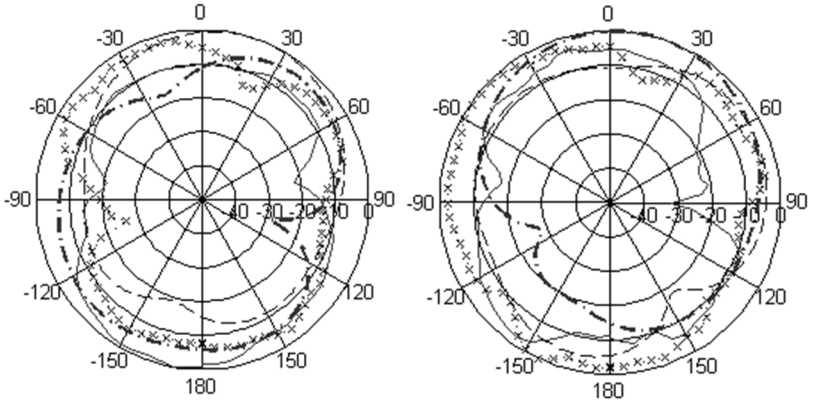

3: (D1 OFF, D2 ON) state at 4.2 GHz

(a) (b)

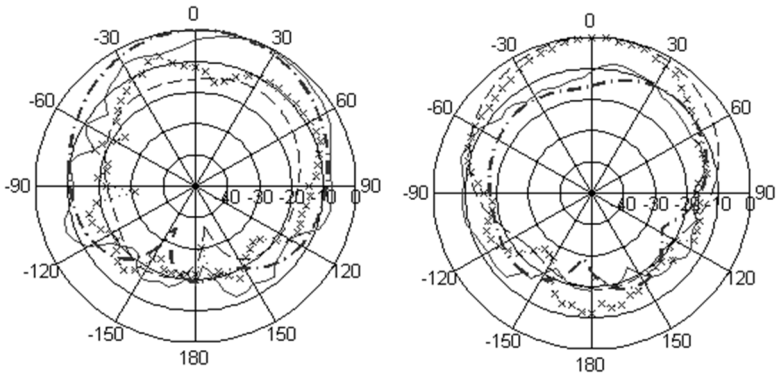

4: (D1 OFF, D2 ON) state at 5.1 GHz

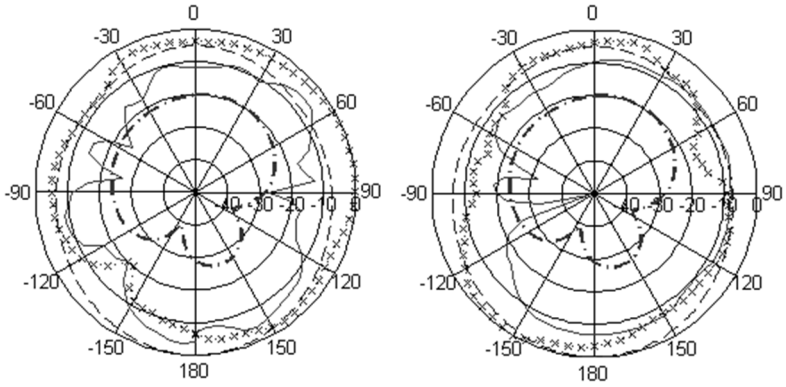

5: (D1 ON, D2 OFF) state at 3.3 GHz

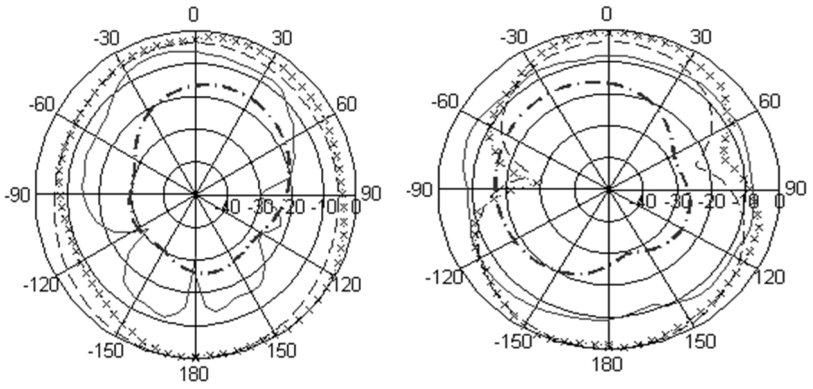

6: (D1 OFF, D2 OFF) state at 3.2 GHz

(a) (b)

Fig. 11: Simulated and measured radiation patterns in the four states: (a) yz-plane and (b) xz-plane. Simulated E_φ: dashed line, simulated E_θ: dash/dotted line, measured E_φ: "×-×-×" and measured E_θ: solid line.

Fig. 11 shows the radiation patterns of the antenna in the four states, which indicate the suitability of the designed antenna for WiMAX and WLAN applications. Variations between the simulated and measured results may arise due to the connection of the antenna to the non-ideal absorber by coaxial cable in the anechoic chamber.

v. Simulated and Measured Gains:

The simulated and the measured antenna gain as a function of the frequency and at four states of the two diodes are shown in Fig. 12. The measured gain values were taken at the resonance frequencies of each switched state.

From the different results shown in sub-section V, it can be observed that the antenna exhibits a good maximum gain of about 5.8 dB at (D1 OFF, D2 OFF), 2.5 dB at (D1 ON, D2 OFF) and 3.0 dB at (D1 ON, D2 ON) states around the 5.1-5.4 GHz band. Furthermore, it has a maximum gain of approximately 3 dB in the (D1 ON, D2 OFF) state at 3.3 GHz with a lower value of 0.4 dB at 4.25 GHz. This enhances the performance of the antenna at providing up to ten different frequency bands between 2 to 6 GHz with relative impedance bandwidths of around 2.5% and 8%. Moreover, the bandwidths in the (D1 OFF, D2 ON) state cover the unlicensed ISM (2.4 - 2.48 GHz) band used in IEEE 802.11b/g, and the U-NII

(5.15-5.35 GHz) band used in IEEE 802.11a for WiMAX and Wi-Fi applications. The (D1 ON, D2 OFF) and (D1 OFF, D2 OFF) states allow operation in other WiMAX application bands. The (D1 ON, D2 ON) state can cover LTE and UMTS bands, for defence and security applications.

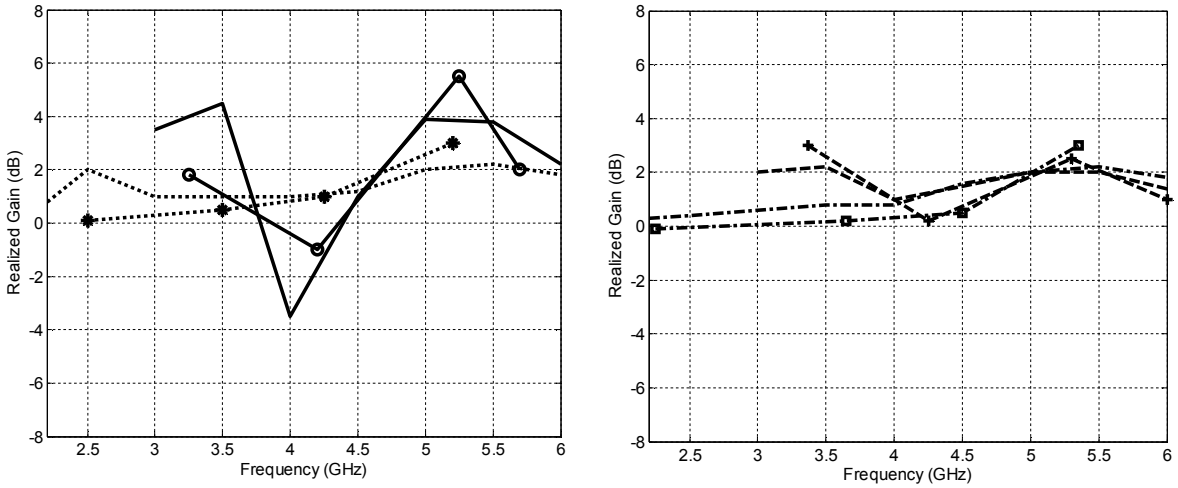

(a) (b)

Fig. 12. Simulated and measured realized gains for the four states:
a) (D1 OFF, D2 OFF) simulated: solid line and measured solid with circles and (D1 OFF, D2 ON) simulated dotted line, measured simulated with stars
b) (D1 ON, D2 OFF) simulated dashed line and measured dashed line with plus symbols (D1 ON, D2 ON) simulated dotted/dashed line and measured dotted/dashed line with square symbols.

Variations between the measured and simulated results may arise owing to losses in the biasing circuit and the low values of quality factor for the diodes, inductors and capacitors used in building the reconfigurable antenna, thus affecting the values of the measured gain.

IV. CONCLUSION

In this paper, a reconfigurable antenna of compact dimension of $50 \times 45 \times 1.6$ mm^3 is presented and investigated. The design uses a miniaturization technique for the main radiator, including slots for both the patch and ground planes. Multiband operation was achieved by using PIN diodes as switches to reconfigure the antenna, generating specific frequencies for

WiMAX and WLAN applications. As shown in section III, the antenna provides up to ten different frequency bands between 2 GHz and 6 GHz with relative impedance bandwidths of around 2.5% and 8%.

The simulated and measured results for the return loss input resistance and reactance and peak gains in different diode states show acceptable performance for WLAN applications, and the simulated and measured results are in good agreement. The frequency bands obtained from the antenna are potentially suitable for cognitive radio wireless applications.

ACKNOWLEDGMENTS

This work was supported by the Iraqi Ministry of Higher Education and Scientific Research, and by the United Kingdom Engineering and Physical Science Research Council through Grant EP/E022936A.

AUTHORS AFFILIATIONS

Y. I. Abdulraheem, A. S. Abdullah, H. J. Mohammed and R. A. Ali are with Department of Electrical Engineering, College of Engineering, University of Basrah, Iraq.

G. A. Oguntala, R. A. Abd-Alhameed and J. M. Noras are with the School of Electrical Engineering and Computer Science, Faculty of Engineering and Informatics, University of Bradford, West Yorkshire, BD7 1DP, UK.

Corresponding author: r.a.a.abd@bradford.ac.uk

REFERENCES

1. Peroulis, D., K. Sarabandi, and L.P.B. Katehi, *Design of reconfigurable slot antennas.* IEEE Transactions on Antennas and Propagation, 2005. **53**(2): p. 645-654.
2. Ramli, N., et al. *Frequency Reconfigurable Stacked Patch Microstrip Antenna (FRSPMA) for LTE and WiMAX applications*. in *Computing, Management and Telecommunications (ComManTel), 2013 International Conference on*. 2013.
3. Balanis, C.A., *Modern Antenna Handbook*. Balanis, Constantine A. 2008: John Wiley & Sons, Inc.
4. Yuan, Z. and W. Chang-Ying. *An approach for optimizing the reconfigurable antenna and improving its reconfigurability*. in *2016 IEEE International Conference on Signal Processing, Communications and Computing (ICSPCC)*. 2016.
5. Ke, L. and Z. Wang, *Degrees of Freedom Regions of Two-User MIMO Z and Full Interference Channels: The Benefit of Reconfigurable Antennas.* IEEE Transactions on Information Theory, 2012. **58**(6): p. 3766-3779.
6. Hannula, J.M., J. Holopainen, and V. Viikari, *Concept for Frequency Reconfigurable Antenna Based on Distributed Transceivers.* IEEE Antennas and Wireless Propagation Letters, 2016. **PP**(99): p. 1-1.

7. Majid, H.A., et al., *Frequency-Reconfigurable Microstrip Patch-Slot Antenna.* IEEE Antennas and Wireless Propagation Letters, 2013. **12**: p. 218-220.
8. Chaabane, G., et al. *Reconfigurable PIFA antenna using RF MEMS switches*. in *2015 9th European Conference on Antennas and Propagation (EuCAP)*. 2015.
9. Cetiner, B.A., et al., *RF MEMS Integrated Frequency Reconfigurable Annular Slot Antenna.* IEEE Transactions on Antennas and Propagation, 2010. **58**(3): p. 626-632.
10. George, R., C.R.S. Kumar, and S.A. Gangal. *Design of a frequency reconfigurable pixel patch antenna for cognitive radio applications*. in *2016 International Conference on Communication and Signal Processing (ICCSP)*. 2016.
11. Oh, S.S., et al. *Frequency-tunable open-ring microstrip antenna using varactor*. in *Electromagnetics in Advanced Applications (ICEAA), 2010 International Conference on*. 2010.
12. Li-Rong, T., et al., *Ferrite-Loaded SIW Bowtie Slot Antenna With Broadband Frequency Tunability.* IEEE Antennas and Wireless Propagation Letters, 2014. **13**: p. 325-328.
13. Chen, G., X.l. Yang, and Y. Wang, *Dual-Band Frequency-Reconfigurable Folded Slot Antenna for Wireless Communications.* IEEE Antennas and Wireless Propagation Letters, 2012. **11**: p. 1386-1389.
14. Perruisseau-Carrier, J., P. Pardo-Carrera, and P. Miskovsky, *Modeling, Design and Characterization of a Very Wideband Slot Antenna With Reconfigurable Band Rejection.* IEEE Transactions on Antennas and Propagation, 2010. **58**(7): p. 2218-2226.
15. Symeon, N., et al., *Pattern and frequency reconfigurable annular slot antenna using PIN diodes.* IEEE Transactions on Antennas and Propagation, 2006. **54**(2): p. 439-448.
16. Stepan Lucyszyn, a.S.P., *RF MEMS for Antenna Applications* in *7th European Conference on Antennas and Propagation (EUCAP 2013)* EurAAP, Editor. 2013, EurAAP: Gothenburg, Sweden. p. 1988-1992.
17. Majid, H.A., et al. *Frequency reconfigurable square ring slot antenna*. in *2015 IEEE International RF and Microwave Conference (RFM)*. 2015.
18. Hum, S.V., M. Okoniewski, and R.J. Davies, *Modeling and Design of Electronically Tunable Reflectarrays.* IEEE Transactions on Antennas and Propagation, 2007. **55**(8): p. 2200-2210.
19. Weily, A.R., T.S. Bird, and Y.J. Guo, *A Reconfigurable High-Gain Partially Reflecting Surface Antenna.* IEEE Transactions on Antennas and Propagation, 2008. **56**(11): p. 3382-3390.
20. Medeiros, C.R.C., A. ; Costa, J.R. ; Fernandes, C. A., *Evaluation of Modelling Accuracy of Reconfigurable Patch Antennas*, in *Proceeding, Conference on Telecommunications - ConfTele*, I.d. Telecomunicações, Editor. 2007, Instituto de Telecomunicações: Peniche, Portugal, .